In situ imaging of electromigration-induced nanogap formation by transmission electron microscopy

Hubert B. Heersche,[a] Günther Lientschnig,[b] Kevin O'Neill,
Herre S. J. van der Zant, and Henny W. Zandbergen
Kavli Institute of Nanoscience, Delft University of Technology, P.O. Box 5046, 2600 GA, Delft, The Netherlands

(Received 11 May 2007; accepted 30 June 2007; published online 17 August 2007)

The authors imaged electromigration-induced nanogap formation *in situ* by transmission electron microscopy. Real-time video recordings show that edge voids form near the cathode side. The polycrystalline gold wires narrow down until a single-grain boundary intersects the constriction along which the breaking continues. During the last 50 ms of the break, a relatively large deformation of the constriction's geometry occurs. The shape of the anode (blunt) and the cathode (sharp) is asymmetric when the wire breaks with a bias voltage applied, but symmetric when a narrow constriction breaks spontaneously. © *2007 American Institute of Physics*.
[DOI: 10.1063/1.2767149]

Electromigration has been used as a fabrication technique[1] for closely spaced electrodes that can serve as contacts for single molecules and nanocrystals.[2] Several studies have worked on feedback mechanisms, based on resistance monitoring, to control the electromigration process and create smaller gaps.[3] Although resistance measurements can give an indication of the separation between the electrodes[4] they do not provide a reliable method of characterizing nanogaps. Recently, the resulting gap geometry after electromigration has been imaged *ex situ* using transmission electron microscopy (TEM) by Strachan *et al.*[5] They find clean (debris-free) ~5 nm nanogaps that relax to about 20 nm over time (months).

Here, we study the *dynamics* of the nanogap formation. For this purpose, we imaged the electromigration process *in situ* with TEM. In contrast to scanning electron microscopy,[6] TEM has a sufficiently high resolution to study electromigration on a nanometer scale. We started by fabricating thin (12 nm) gold wires with small constrictions on top of transparent Si_3N_4 membranes. To contact the wires electrically while monitoring them by TEM, the junctions were mounted in a homebuilt TEM holder with wire feedthrough. Si_3N_4 membranes were obtained commercially. They consist of 30×30 μm^2 Si_3N_4 (20 nm thick) windows etched out of Si/Si_3N_4 wafers [Fig. 1(a)]. Thin gold wires were first evaporated on top of the membrane without using an adhesion layer. In a second fabrication step, the thin wires were contacted by 100 nm thick leads and bonding pads. The total device resistance was 600–800 Ω. A small piece of wafer containing a membrane window and the patterned wiring was then glued onto a small printed circuit board (PCB) and wire bonded. The sensitivity of the devices to electronic discharging complicated the experiments. The design of the TEM holder was such that primary electrons do not hit the PCB or glue, preventing contamination. A Philips CM300UT-FEG electron microscope was used and video data were recorded with 20 images/s. The resulting recordings are available online.[7]

Wires were electromigrated using either a passive breaking scheme (1 device) or an active breaking scheme with resistance feedback (3 devices). In the passive scheme, a voltage is ramped over the junction while the current is monitored until the junction breaks (typically the electromigration process starts at a few milliamperes). To slow down the breaking process,[3] we also developed an active scheme in which a computer program ramps the voltage until either the resistance rises above a threshold or a maximum voltage is reached, whereupon the voltage is returned to zero and the ramp is started over. The cycle time is 25–50 ms. Upon electrically stressing the wire with 1–2 mA, a reversible resis-

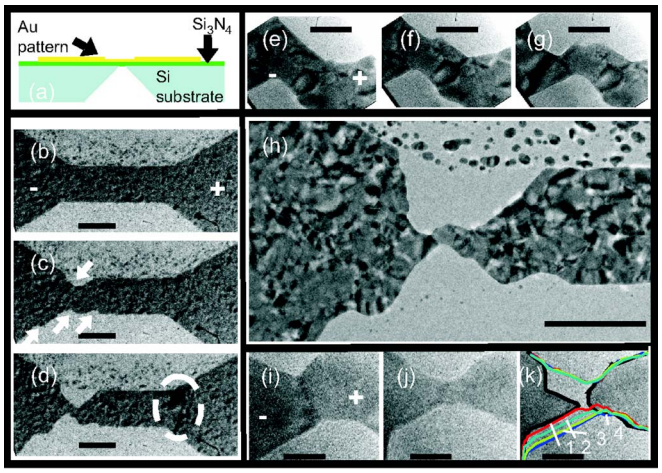

FIG. 1. (Color online) (a) Sample schematic (cross section). [(b)–(l)] Passive breaking of a 12 nm thick Au wire by ramping a bias voltage. (b) Initial (polycrystalline) device before breaking. (c) Voids form at the cathode side of the wire (arrows). (d) Hillocks can be observed at the anode side (circle). [(e)–(g)] The wire narrows down further until a single-grain boundary spans the width of the constriction. (h) High resolution overview. [(i)–(k)] The thick black line in (k) indicates the shape of the gap. The line numbers 1–4 in (k) correspond to the shape of the wire in (j) and three images frames 100, 200, and 300 ms earlier, respectively. The wire finally breaks along the grain boundary with a final gap size of 6 nm. Scale bars correspond to 200 nm [(b)–(d), and (h)], 40 nm [(e)–(g)], and 20 nm [(i)–(k)]. The arrows indicate grain boundaries.

[a]Electronic mail: h.b.heersche@tudelft.nl
[b]Present address: Nanotechnology Research Institute, National Institute of Advanced Science and Technology, 1-1-1 Umezono, Tsukuba, 305-8568 Japan, and JST-CREST.

 © 2007 American Institute of Physics
Downloaded 10 Aug 2010 to 131.180.130.114. Redistribution subject to AIP license or copyright; see http://apl.aip.org/apl/copyright.jsp

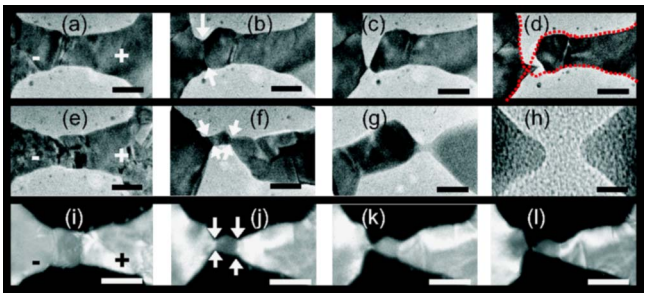

FIG. 2. (Color online) Active breaking of three devices (three rows, respectively). [(a), (e), and (i)] Frames show the wires before electromigration, [(b), (f), and (j)] the initial stage of the electromigration in which grains fuse and voids start to form along grain boundaries, [(c), and (k)] the last frame before breaking occurs, [(d), (l)] and the corresponding subsequent frame, (sampling frequency of 20 Hz). The contour of (c) is indicated in (d) by a red dotted line. After frame (g), the active breaking was stopped and the device broke without a current applied (h). Frames [(i)–(l)] were taken in dark field mode. Scale bars correspond to [(a)–(e) and (i)–(l)] 50 nm, (f) 25 nm, (g) 10 nm, and (h) 5 nm. Arrows indicate grain boundaries.

tance increase of about 10% was observed which can be attributed to heating. Upon increasing the current, the resistance did not increase significantly further until the wires broke abruptly and the resistance became infinite.

We first discuss the breaking of a polycrystalline gold wire [Fig. 1(b)] using the passive breaking scheme. The bridge is initially 200 nm wide and 600 nm long with a distribution of grain sizes up to about 50 nm. We interrupted the breaking twice, by ramping the bias voltage quickly to zero, in order to zoom in on the region of interest. Figures 1(b)–1(d) correspond to the first ramp. Four voids appear at different locations near the cathode [indicated by arrows in Fig. 1(c)], strikingly not only at the narrowest part of the wire. In Fig. 1(d), a dark area can be observed near the anode (dotted circle), indicating the deposition of material forming a hillock.

After changing to a higher magnification, the electromigration process was continued [see Figs. 1(e)–1(g)]. Grain boundaries rearrange as the shape of the constriction changes. Figure 1(h) shows an image of the constriction formed after the second interruption of the breaking process. A zoom in on the grain boundary that separates the constriction is shown in Fig. 1(i). Failure occurs when the wire is about 15 nm wide on a time scale shorter than our sampling time [50 ms, Figs. 1(j) and 1(k) are consecutive frames]. The resulting gap is about 5 nm and the electrode shape is asymmetric: the cathode side of the gap has a relatively sharp pointlike shape whereas the anode side is more rounded.

Figures 2(a)–2(l) show the active breaking of three different samples in bright field, bright field, and dark field imaging modes, respectively. The width of the lithographically defined constrictions is 50 nm and the length is about 200 nm. Grain boundaries span the width of the constriction (transgranular or bamboo wires). In the active scheme each break has been performed in a 30 s to 2 min time span. The void formation occurs along grain boundaries [indicated by arrows in Figs. 2(b), 2(f), and 2(j)] at the cathode side of the wire and proceeds as in the last stage of the breaking in Fig. 1. Just before the void formation starts, several grains fuse and larger grains are formed. The process is preceded by a movement of a grain boundary in the direction of electron flow. In Fig. 2(c), the constriction has become so small that a bridge of only a few nanometers connects the two electrodes. The consecutive frame [see Fig. 2(d)] shows the formation of a gap. A remarkably rapid deformation of the electrodes—of the order of 10^5 atoms have been transported in the last 50 ms compared to 10^2 atoms in the 50 ms before—has occurred during this final stage of the breaking. Comparing the constriction's shape just before [red dashed line in Fig. 2(d)] and after breaking even suggests backflow of material toward the cathode. The cathode side of the electrode has again a pointlike shape (radius $\sim$1 nm) whereas the anode side is flat. The final gap is 6 nm.

The gap formation process in another device [Figs. 2(e)–2(h)] is similar except that we stopped the electromigration process, by reducing the bias voltage to zero, when the wire became as narrow as 2 nm. At that point, the wire broke spontaneously within 15 s with no bias voltage applied. The remaining gap is 5 nm. Note the symmetric shape of the contacts after the spontaneous break, in contrast to the asymmetric shape that was observed in samples that broke with an applied bias. We imaged the breaking of another wire in dark field mode [Figs. 2(i)–2(l)], in which the contrast depends strongly on the orientation of the grains. The breaking follows the same pattern as for the other two transgranular wires.

Electromigration theory differentiates between two regimes depending on the ratio between grain diameter D and wire width W. Initially, the sample in Fig. 1 is in the polycrystalline regime ($W \gg D$), where mass transport is mediated mainly by surface and grain boundary diffusion. This results in voids [Fig. 1(c)] and associated hillocks [Fig. 1(d)]. Since momentum transfer between electrons and gold ions (wind force) dominates the direct force of the electric field, which is in the opposite direction, voids are expected to form at the cathode side of the wires, as is observed in our experiment.

In the final stage of the breaking, all wires have become transgranular, i.e., one grain boundary intersects the whole wire width ($W \leqslant D$). The grain boundary that divides the wire forms the bottleneck for mass transport and the wire narrows down along it. This in contrast to studies in Al lines where intragranular voids have been observed.[8] The large deformation [Figs. 1(k) and 2(d)] during the last 50 ms of the breaking is unexpected. It suggests that the electron wind force, which is the driving force for mass transport throughout the breaking process, no longer dominates at the very last moment of breaking. Mechanical stress can also be excluded as a driving force, since the deformations are very local.

The fact that the grain boundary along which the final breaking occurs remains visible until a gap has formed indicates that electromigration and not melting is the cause of the nanogap formation. The final gap size in our experiments is 5–6 nm, similar to previous findings[5] when using silicon nitride membranes, but larger than in experiments on different substrates.[3] This gap size also holds for the spontaneous break described above, excluding higher temperatures at the moment of breaking (i.e., due to the lower thermal conductance of the silicon nitride substrate) as an explanation for this difference. A difference in interaction of the gold atoms with the Si_3N_4 surface in the present experiment compared to SiO_2 or Al_2O_3 substrates in previous work is the most likely explanation.

A possible reason for the dramatic shape change in the last 50 ms is that the direct force of the electric field, which becomes very high near the gap at the instant the wire

Downloaded 10 Aug 2010 to 131.180.130.114. Redistribution subject to AIP license or copyright; see http://apl.aip.org/apl/copyright.jsp

breaks, results in a quick deformation of the electrodes[9] [Figs. 1(k) and 2(d)] and a in backflow of material [Fig. 2(d)]. The effect of the electric field could also explain the difference in electrode shape which is asymmetric [blunt anode and sharp cathode, Figs. 1(k) and 2(d)] or symmetric [Fig. 2(h)] after breaking with and without voltage bias applied, respectively.

The authors thank Edgar Osorio for help with the experiment and acknowledge our debt to the Dutch Fundamenteel Onderzoek der Materie (FOM) for financial support. One of the authors (K.O.) was supported by the Marie Curie Fellowship Association.

[1]H. Park, A. K. L. Lim, A. P. Alivisatos, J. Park, and P. L. McEuen, Appl. Phys. Lett. **75**, 301 (1999).
[2]H. Park, J. Park, A. K. L. Lim, E. H. Anderson, A. P. Alivisatos, and P. L. McEuen, Nature (London) **407**, 57 (2000); J. Park, A. N. Pasupathy, J. I. Goldsmith, C. Chang, Y. Yaish, J. R. Petta, M. Rinkoski, J. P. Sethna, H. D. Abruna, P. L. McEuen, and D. C. Ralph, *ibid.* **417**, 722 (2002); W. J. Liang, M. P. Shores, M. Bockrath, J. R. Long, and H. Park, *ibid.* **417**, 725 (2002); L. H. Yu, Z. K. Keane, J. W. Ciszek, L. Cheng, M. P. Stewart, J. M. Tour, and D. Natelson, Phys. Rev. Lett. **93**, 266802 (2004).
[3]G. Esen and M. S. Fuhrer, Appl. Phys. Lett. **87**, 263101 (2005); D. R. Strachan, D. E. Smith, D. E. Johnston, T. H. Park, M. J. Therien, D. A. Bonnell, and A. T. Johnson, *ibid.* **86**, 043109 (2005); A. A. Houck, J. Labaziewicz, E. K. Chan, J. A. Folk, and I. L. Chuang, Nano Lett. **5**, 1685 (2005).
[4]M. F. Lambert, M. F. Goffman, J. P. Bourgoin, and P. Hesto, Nanotechnology **14**, 772 (2003).
[5]D. R. Strachan, D. E. Smith, M. D. Fischbein, D. E. Johnston, B. S. Guiton, M. Drndic, D. A. Bonnell, and A. T. Johnson, Nano Lett. **6**, 441 (2006).
[6]T. Taychatanapat, K. I. Bolotin, F. Kuemmeth, and D. C. Ralph, Nano Lett. **7**, 652 (2007).
[7]See EPAPS Document No. E-APPLAB-91-004731 for video recordings. This document can be reached via a direct link in the online article's HTML reference section or via the EPAPS homepage (http://www.aip.org/pubservs/epaps. html).
[8]J. H. Rose, Appl. Phys. Lett. **61**, 2170 (1992).
[9]T. M. Mayer, J. E. Houston, G. E. Franklin, A. A. Erchak, and T. A. Michalske, J. Appl. Phys. **85**, 8170 (1999).

Downloaded 10 Aug 2010 to 131.180.130.114. Redistribution subject to AIP license or copyright; see http://apl.aip.org/apl/copyright.jsp